Available online at www.sciencedirect.com
ScienceDirect
Diamond & Related Materials 16 (2007) 1053–1057
DIAMOND AND RELATED MATERIALS
www.elsevier.com/locate/diamond

Electronic performance of 2D-UV detectors

G. Mazzeo [a], S. Salvatori [a,*], G. Conte [a], V. Ralchenko [b], V. Konov [b]

[a] Department of Electronic Engineering, University of Rome "Roma Tre", Via della Vasca Navale, 84-00146 Rome, Italy
[b] General Physics Institute of Russian Academy of Sciences, 38 Vavilov Street, 119991, Moscow, Russia

Available online 29 January 2007

Abstract

With the aim of contributing to the development of two-dimensional UV and X-ray detectors, also stimulated to evaluate specific amplification, handling and addressing electronics, we present a 16-pixel matrix sensor based on high quality polycrystalline diamond. Thick polycrystalline diamond specimens, in the 0.2–0.6 mm range, have been used for the tests and the development of the prototype. Crossed 1 mm large chromium strips have then been realized by lithography on the metal deposited on both the two sample surfaces. The single pixel structure of a matrix appears like a metal-diamond-metal vertical device with a volume which is directly related to the diamond thickness (0.2–0.6 mm^3).

Initially, to evaluate the sensor-grade quality of the diamond films, each pixel has been characterized by means of: *I–V* characteristic in the dark and under ns pulsed excimer laser irradiation; linearity with the photon flux; spectral photoresponse in the 200–1000 nm range. The lateral charge collection at the non-illuminated sensing elements has also been measured to estimate the cross-talk between pixels. Successive tests have been devoted to study the whole matrix response by addressing the pixels singly through the realized electronics both in CW and chopped monochromatic UV illumination. The implemented low-noise transimpedance amplifiers (1 V/1 nA) showed a good linearity whereas the bandwidth was limited just to 20 Hz. Finally, the intensity distribution of a 1×1 cm^2 monochromatic UV beam, extracted by a xenon discharge lamp source, as acquired by a realized prototype is illustrated and analyzed.

Keywords: UV photodetector; CVD-diamond; Two-dimensional sensor

1. Introduction

The interest in high-performance photodetectors for operation in the UV regions of the spectrum is growing fast. This arises from the increasing industrial use of intense excimer laser sources which are proving to be highly successful for fabricating components with feature sizes in the 0.05–1000 μm range [1,2]. Spanning the areas that include MEMS technology and ULSI photolithography, such industrial components respond to the critical features nowadays imposed by electronics and telecommunications. The optimal use of the radiation in such application fields requires not only the knowledge of position and impinging intensity of the beam but also its profile. As the sources, high-performance sensors to be used for laser beam diagnostics are receiving the necessary attention from most research groups.

Together with interesting physical properties such as the high cohesive energy and thermal conductivity of diamond, the availability of large area deposits together with the possibility of reducing the surface roughness and enhancing of the electronic properties by mechanical removal of the nucleation and growth layers is leading to the possibility of implementing very complex contact structures on diamond. Nowadays, its unique combination of chemical and physical properties makes diamond extremely attractive for use as photon and particle detectors. Diamond devices have potential applications in very high rate radiation fields, such as deep-UV excimer lasers photolithography [3,4] but also in high voltage X-ray beams metrology [5]. Moreover, position sensitive detectors have been already proposed and tested [6,7] and one- and two-dimensional devices for UV imaging have been also introduced [8,9].

Thus diamond shows excellent physical properties for the realization of many kind of devices, technological limitations hinder the complete exploitation of the mentioned characteristics. In the field of the photon and particle detection, the main problems are still related to the doping difficulties. For single pixel detectors this limitation can be readily overcome thanks to the high dark resistivity of the material, that can be as high as 10^{13} Ω cm. As a

* Corresponding author. Tel.: +39 0655177091; fax: +39 065579078.
E-mail address: salvator@uniroma3.it (S. Salvatori).

0925-9635/$ - see front matter © 2006 Elsevier B.V. All rights reserved.
doi:10.1016/j.diamond.2006.11.101

consequence, very high detectivity can be obtained for photoconductive devices, that don't require any doping. This approach has been followed by many research groups and excellent performances in terms of responsivity, detectivity, rejection of subgap radiation, and response speed have been obtained [4,10,11]. These performances have been proved for UV, X-ray and particle detection, thus covering all the fields where diamond might introduce significant improvement with respect to other conventional semiconductors. Nevertheless, problems are found when trying to extend this design to a multi-pixel two-dimensional device. Thus many progresses are being made in the field of diamond transistors [12], this technology is still far from the maturity necessary to implement the addressing circuitry directly on diamond. It is then necessary to use a hybrid technology, with a conventional silicon readout circuit connected to the diamond detector. The flip chip hybridization, the most used for 2D arrays, already implemented for example in quantum well infrared photodetectors, consists in the facing of the two chips and the connection of each detector to the silicon front-end electronics via an indium bump. Very high link density and reliability can be obtained, and the feasibility with diamond detectors has been shown [13]. Nevertheless, some issues are related to this technology: the most important for the applications explored in this paper is that the radiation that isn't absorbed by the diamond detector can reach the silicon readout circuit. For UV detection this may be the visible and near ultraviolet radiation that, absorbed by the silicon, can reduce the visible blindness of the entire system, while in the field of high energy radiation the readout chip can be damaged absorbing the radiation.

The approach we adopted during this work consists in the realization of contact strips on the two surfaces of the detector oriented along the x and y directions, respectively. At each ideal crossing of two strips, a photoconductor with a sandwich contact structure is formed. The individual photosensor signal is measured by connecting the correspondent column to the biasing voltage and measuring the photogenerated current flowing in the row which is connected to the ground. With this scheme, all the switching, biasing and amplifying circuitries are off axis with respect to the incident beam as required for the detection of high energy radiation or particles. The most important details and specifications used to design such a photosensing system are discussed in the next section.

2. Conditioning electronics requirements and architecture

Fig. 1(a) depicts the diamond sensor contact structure mentioned above. Black strips represent the contact realized on the growth side of the film, whereas grey colour is used to depict the four contacts deposited on the opposite nucleation side of the same specimen.

With the typical intensities of UV or X-ray beams, a photocurrent of the order of magnitude of the pA is to be expected at each pixel. Besides the sandwich structure of the sensor, together with the relatively high thickness of the diamond film, necessary to obtain the needed quality and mechanical stiffness, a high polarization voltage has to be used to increase the charge collection efficiency of the detector. Indeed, assuming charge transport below the saturation velocity, from the expression of the internal quantum efficiency [14]

$$\eta = \frac{V\mu\tau}{d^2},$$

where μ is the mobility, τ the carrier lifetime, V the applied voltage and d the sensor thickness, assuming 600 μm for the film thickness and a typical $\mu\tau$ product around 10^{-7} cm^2/V [15], we can predict a collection efficiency value around 0.3% at 100 V. Higher polarization voltage may increase this value (that for photoconductors can even be greater than one) without incurring the problem of breakdown, but it would require specific electronics. For this reason this value has been chosen as the maximum. Four independent optocouplers can be used to connect the bias source to the sensor columns. A column can be biased enabling the corresponding optocoupler leaving float the others. To scan all the sensing area, an enable sequence can be adopted switching the bias along all the columns.

Considering the expected low current signal amplitude, a scheme with one amplifier per row is the only possible choice as commercially available analog switches show leakage currents higher, or at least comparable, to the useful signal. The choice is then on parallel amplification of all the row currents by independent transimpedance amplifiers. To simplify the measuring system, we multiplexed the amplifier outputs towards a precision millivoltmeter (Keithley, mod. 2000 Multimeter). Anyway, to increase the system response speed, a simultaneously probing of

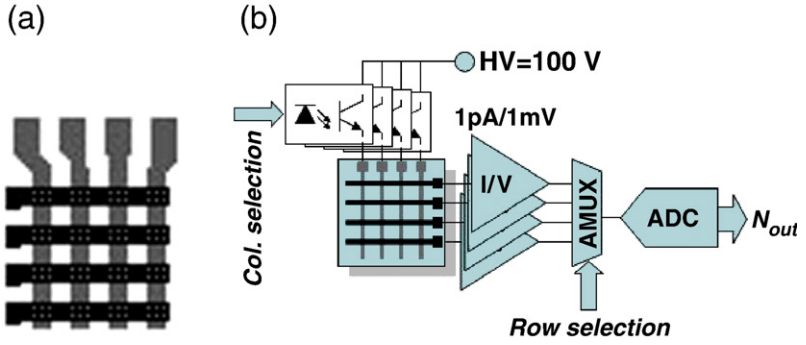

Fig. 1. In (a), the sensor contact structure is shown as the superposition of the row-strips on the growth side (black) and column-lines on the nucleation side (grey) of the diamond sample. The block diagram of the conditioning electronics is reported in (b). The high voltage bias is switched between columns via four optocouplers. The photocurrent signals at each row are conditioned by four transimpedance amplifiers (based on the precision TLC374 quad operational amplifier).

the outputs is preferred via independent analog to digital converters of the acquiring circuitry.

The principle of operation of such a conditioning electronics is summarised in Fig. 1(b) where a block representation has been used to depict the system. Based on the precision quad operational amplifier TLC274 (from Texas Instruments), four transimpedance amplifiers, with feedback resistors of 1 GΩ, allow to convert the input current in an output voltage with a 1 V per 1 nA gain. The four outputs are interfaced to the A/D converter or the voltmeter by an analog multiplexer. The high voltage used to enhance the pixel sensitivity is applied to the detector columns via a TLP627 optocoupler (from Toshiba). Column biasing and output signal row selections are PC-controlled by a dedicated digital interface circuitry.

3. Experimentals and material characterization

Sensor-grade, 0.3–0.6 mm thick, 1 cm^2 large, polycrystalline diamonds deposited by microwave-assisted CVD technique were used for the present work. In order to obtain excellent mirror-like surfaces, with a roughness lower than 8 nm, a mechanical-polishing treatment was performed on both the growth and nucleation sides of the specimen. Tens of microns are removed by the samples, enhancing the electronic properties at both the two sides of the films. By this way, no particular differences are expected on the detector sensitivity symmetry with respect to electrons or holes transit. Anyway, careful investigations of such terms are in progress for the future. Standard photolithographic technique was adopted on evaporated chromium to create the contact structure illustrated in Fig. 1(a): 1 mm wide strip lines, separated by a space of 1 mm. Six holes have been also realized to allow the light absorption into the diamond bulk as required by the sandwich structure of the detector.

The current-to-voltage characteristics of each pixel showed an ohmic nature and the estimated dark resistivity was of 10^{11} Ω cm. As shown in Fig. 2, the response speed under pulsed UV irradiation was measured by means of a 193 nm excimer laser (Neweks, PSX 100, filled with an ArF mixture, FWHM = 5 ns, 2.5 mJ of pulse nominal energy) revealing that the sample is able to follow the excitation in such a time scale. The quality was also indicated by the power-law dependence on the impinging energy with the exponent around 0.5 at the highest photon fluxes [4].

Finally, at each pixel, the steady state spectral response of the devices was measured over the 180–1000 nm range by means of the monochromatic light sourced by a xenon discharge lamp and a SPEX 1680B Double Spectrometer. The typical results are reported in the inset of Fig. 2, which show the sharp diamond band edge at 5.5 eV and a good UV/visible discrimination of the detectors. Samples can show excellent performances (curve a) [16] although for the UV–visible discrimination can decrease down to 100 in lower quality films (curve b).

4. Front-end electronics main performances

The prototype was preliminarily tested evaluating the performances of the front-end circuitry as revealed by directly

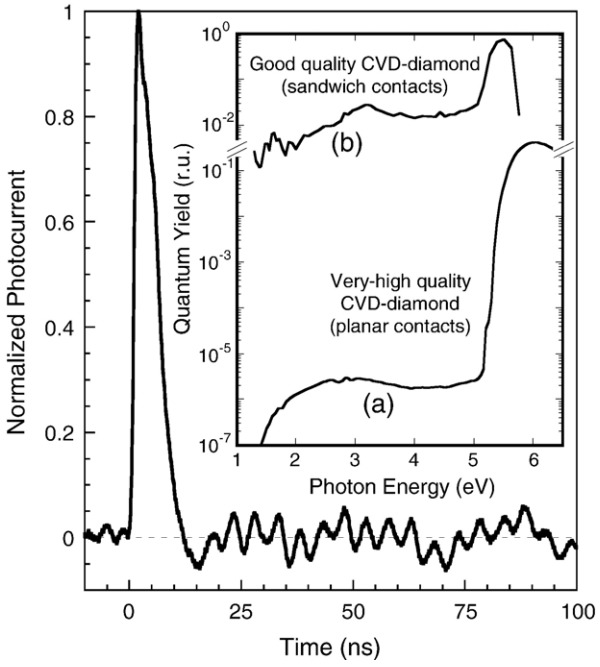

Fig. 2. CVD diamond photoresponse under pulsed excimer laser excitation in the ns time regime. The typical quantum efficiencies of CVD diamond samples are reported as inset. For a very high quality film (curve a), best performances have been detected for the planar configuration of the contacts [15]. The band edge photoresponse is clearly evidenced as an increase on the efficiency for photon energy greater than the diamond band-gap and a visible–UV discrimination is evidenced. A lower detection UV–visible discrimination can be found for lower quality films (curve b).

injecting a known current into the transimpedance amplifiers inputs generated by a precision Keithley 6221 DC and AC current source (0.1 pA of resolution). The performed measurement shows an excellent linearity and a very low gain error, lower than 1%, for all the amplifiers simply induced by the tolerance of the feedback resistors. In addition, for a very low input current amplitude, the leakage at the amplifier input and on the circuit board may dominate and introduce some non-ideal behavior. In our case, no evidence of a deviation of the transfer function from the linear behavior has been found. The unavoidable experimental points scattering we found has been best attributed to the noise on the output signal. Such a noise can be then considered as the main limitation to the minimum detectable signal amplitude, ΔI, we can evaluate by:

$$\Delta I = \frac{\sigma}{A}$$

where A is the system amplification and σ is the standard deviation of the output signal, which depends on the bandwidth used for the measurements. This noise has been estimated by measuring the standard deviation of the output spread when the amplifier input is left afloat. With a bandwidth of 5 Hz of the measuring instrument (Keithley, mod. 2000 Multimeter), a minimum detectable signal of 0.1 pA has been evaluated. An analysis of the noise spectrum would help in pointing out the noise sources.

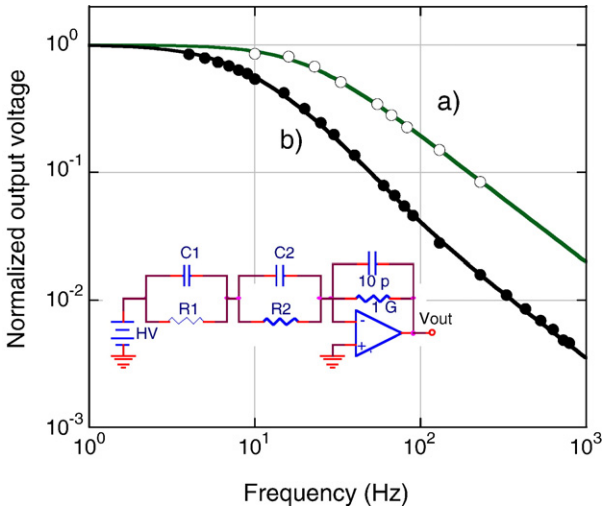

Fig. 3. Normalized output signal of the conditioning electronics as a function of the frequency of the input current signal. Data of curve (a) are obtained by means of a current source Keithley 6221, whereas curve (b) refers to the case of a connected diamond sample illuminated by a weak UV chopped light. The equivalent scheme refers to the case in which the optocoupler is used for pixel biasing. Continuous lines represent best fit results (see text).

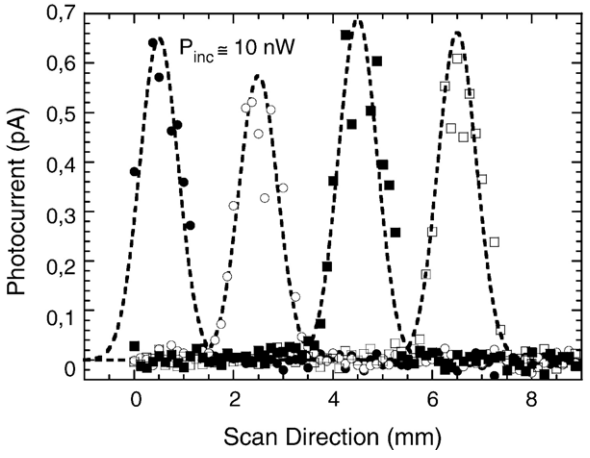

Fig. 4. Amplitude of the output signal when a 1 mm^2 beam illuminates the pixels along the row direction. An output signal is detected only when light illuminates the biased pixel revealing a very low cross-talk between pixels. Dotted lines are guides for the eye.

At last we report, in Fig. 3 (curve a), the frequency response of the amplifier. As expected the transcharacteristic is a single-pole function (continuous line) with a cut-off frequency around 20 Hz. Such a low cut-off value is mainly induced by the presence of the capacitor we inserted into the transimpedance amplifier feedback path: the bandwidth reduction is the drawback to pay to assure the adequate phase margin for the stability of the system and the sufficient signal-to-noise ratio for the output.

5. Preliminary measurements

To evaluate the detection performances of the array, the sample was irradiated by the weak UV light (220±10 nm) sourced by a xenon lamp filtered through a monochromator.

The dynamic photoresponse was measured under chopped light condition at a variable frequency in the 3–1000 Hz range. The detector output signal, conditioned by the dedicated front-end electronics, shows the behavior depicted in Fig. 3 (curve b). As a rough estimation, the whole detection system shows a main cut-off frequency around 10 Hz, slightly lower than that found for the conditioning electronics alone, indicating a decrease of the system response speed mainly due to the parasitic elements introduced by the pixel biasing circuit (optocoupler) instead of the diamond sample. Indeed, according to the equivalent scheme reported in Fig. 3, best fit result of experimental data (continuous line) states the presence of an R_1C_1 element in series to that of a pixel (R_2C_2) whose contribution appears as the addition of one pole (around 7 Hz) and one zero (at about 74 Hz) to the pole contribution of the transimpedance amplifier (1 GΩ × 10 pF). Diamond high speed photoresponse revealed under excimer laser pulsed excitation may allow working at higher chopping frequency and would then require a faster response of the transimpedance amplifier and biasing circuitry which have to be redesigned for the specific application.

Maintaining a fixed bias on one column, the cross-talk between pixels has been evaluated moving a small incident beam along the rows. To guarantee illuminated pixel signal around the pAmps amplitude, the beam diameter was chosen as 1 mm by means of a circular pin-hole. In this condition, the estimated light power was around 10 nW. The individual output signals on the four rows were recorded as reported in Fig. 4. Being the spot size comparable to the pixel area, signal cannot clearly show the blind region between row contacts. Anyway a good discrimination is evidenced: when the beam impinges the area outside the pixel geometry, the revealed signal is completely masked by the noise amplitude.

Finally, to investigate the feasibility of the two-dimensional beam profiler and aligner system, the detector was illuminated

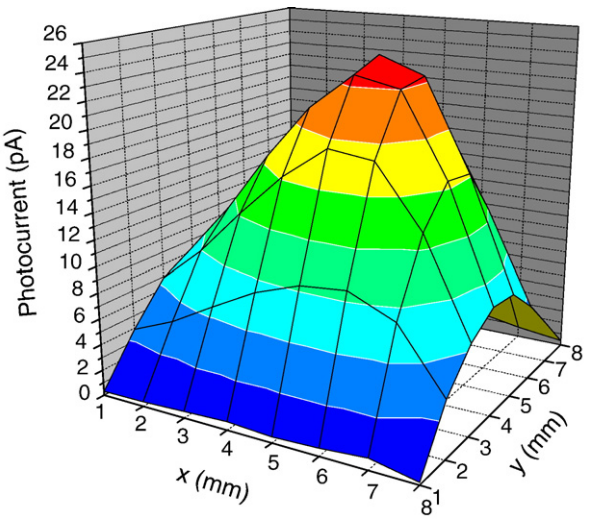

Fig. 5. Beam profile example in the case of a weak UV beam with a cross section around 50 mm^2. Due to the small number of the pixel of the matrix, experimental data have been interpolated to obtain a higher resolution image.

by the monochromatic UV beam having a diameter comparable to the 50 mm^2 sensing active area. To overcome the limitation induced by the poor spatial resolution due to the limited number of pixels, the extracted data have been interpolated and a typical result is shown in Fig. 5 in the case of incidence on the centre of the detector. (This is the case that best represents the operative conditions of the device when used for a beam alignment.) The quality of the obtained result depicts the feasibility of a very efficient imaging system whenever the number of pixel will be increased.

6. Conclusions

A very simple contact structure realized on both the growth and nucleation sides of a thick CVD diamond is proposed as two-dimensional sensing system. A dedicated front-end electronics has been realized for biasing and signal conditioning of the scan-based acquisition system. Even if much work has to be done to enhance the detector spatial resolution and speed photoresponse (by means of higher speed electronics and also by tailoring of diamond characteristics), the realized prototype shows the feasibility of such a proposed 2D scheme for UV and X-ray beam profiler.

References

[1] M. Gower, High-Power Laser Ablation, vol. 3343, SPIE, 1998, p. 171.
[2] Intl. semiconductor roadmap — ITRS, http://www.itrs.net 2005.
[3] M.D. Whitfield, S.P. Lansley, O. Gaudin, R.D. McKeag, N. Rizvi, R.B. Jackman, Diamond Relat. Mater. 10 (2001) 693.
[4] G. Mazzeo, S. Salvatori, M.C. Rossi, G. Conte, M.C. Castex, Sens. Actuators, A, Phys. 113 (2004) 277.
[5] J.P. Negre, C. Rubbelynck, Nucl. Instrum. Methods Phys. Res. A 451 (2000) 638.
[6] G. Mazzeo, G. Prestopino, G. Conte, S. Salvatori, Sens. Actuators, A, Phys. 123–124 (2005) 199.
[7] S. Salvatori, G. Mazzeo, G. Conte, M.C. Rossi, V. Ralchenko, Diamond Relat. Mater. 13 (2004) 948.
[8] S.P. Lansley, O. Gaudin, H. Ye, N. Rizvi, M.D. Whitfield, R.D. McKeag, R.B. Jackman, Diamond Relat. Mater. 11 (2002) 433.
[9] J. Schein, K.M. Campbell, R.R. Prasad, R. Binder, M. Krishnan, Rev. Sci. Instrum. 73 (2002) 18.
[10] A. Mainwood, Semicond. Sci. Technol. 15 (2000) R55.
[11] A. Balducci, M. Marinelli, E. Milani, M.E. Morgada, A. Tucciarone, G. Verona-Rinati, M. Angelone, M. Pillon, Appl. Phys. Lett. 86 (2005) 193509–1.
[12] J.A. Garrido, C.E. Nebel, R. Todt, G. Rösel, M.-C. Amann, M. Stutzmann, E. Snidero, P. Bergonzo, Appl. Phys. Lett. 82 (2003) 988.
[13] W. Adam, C. Bauer, E. Berdermann, P. Bergonzo, F. Bogani, et al., Nucl. Instrum. Methods Phys. Res. A436 (1999) 326.
[14] S.M. Sze, Physics of Semiconductor Devices, Chapt. 13, 2nd ed John Wiley & Sons, New York, 1981.
[15] J.-F. Hochedeza, P. Bergonzo, M.-C. Castex, P. Dhezd, O. Hainaute, et al., Diamond Relat. Mater. 10 (2001) 673.
[16] V.I. Polyakov, A.I. Rukovishnikov, N.M. Rossukanyi, V.G. Ralchenko, F. Spaziani, G. Conte, Diamond Relat. Mater. 14 (2005) 594.